BF-2116
[1-8]

RESEARCH ARTICLE Indian Journal of Animal Research

Knockdown of Anxa2a Expression Causes Hydrocephalus in *Danio rerio*

Suzanna A. Partevian[1#], Ivan N. Rybolovlev[1#], Petr A. Slominsky[1], Maria I. Shadrina[1], Anelya Kh. Alieva[1]

10.18805/IJAR.BF-2116

ABSTRACT

Background: Recently, the number of studies investigating the molecular genetic mechanisms underlying nervous system function in both normal and pathological states has increased significantly. Despite the identification of numerous proteins involved in neural metabolic processes, interest in key regulatory proteins continues to grow. In particular, annexin A2 (ANXA2), previously known for its role in cancer, is gaining attention for its potential role in the development of neurodegenerative diseases.

Methods: This study was conducted on *Danio rerio* of the AB line. Knockdown of the Anxa2a was achieved by microinjection of translation-blocking morpholino oligonucleotides (MOs). The control group was injected with a standard control MO. Phenotypic analysis was performed at 2 days post-fertilization (dpf). Knockdown efficiency was assessed by Western blotting. Relative mRNA levels of target genes (*ahnak*, *egf, egfra, ptena, ptenb, gfap, psen1, psen2*) were determined by real-time PCR.

Result: Phenotypic analysis of the Mo-Anxa2a group across several experimental replicates revealed hydrocephalus (enlargement of the hindbrain ventricle, HBV), as well as eye and olfactory pit deformities. These effects were absent in the control group. Analysis of hydrocephalus severity in morphants identified two subgroups: those with severe and those with mild enlargement of the hindbrain ventricle. Western blotting confirmed a 2-fold reduction in Anxa2a protein levels without a change in its mRNA levels, confirming successful knockdown at the translational level. Furthermore, all groups with Anxa2a knockdown exhibited a statistically significant downregulation of *ptena, ptenb, gfap, psen1* and *psen2*. Notably, in *D. rerio* with severe hydrocephalus, decreased expression of *egf* and *egfra* was also observed, suggesting the involvement of these genes in the pathogenesis of severe hydrocephalus.

Key words: ANXA2, *Danio rerio*, Hydrocephalus, Morpholino oligonucleotides, Nervous system.

Abbreviations: *D. rerio* - *Danio rerio,* dpf - Days post-fertilization, HBV - Hindbrain ventricle, MO - Morpholino oligonucleotides.

INTRODUCTION

Currently, considerable attention is being paid to the study of the molecular genetic mechanisms underlying the functioning of the nervous system under both normal and pathological conditions. In recent years, a large number of genes potentially involved in the development and functioning of the nervous system through various molecular genetic mechanisms have been identified; however, the roles of individual genes often remain unclear (Mawolo and Akiti, 2021).

One such gene is ANXA2. This gene encodes annexin A2 (ANXA2), a protein involved in processes such as vesicular transport, receptor activation, membrane remodeling, cytoskeleton organization, cell division and mRNA transport (Bharadwaj *et al.,* 2013, Grindheim *et al.,* 2017, Partevian *et al.,* 2025). The role of this protein in the development of pathological processes in the nervous system is being actively studied (Rudenok *et al.,* 2022, Zhang *et al.,* 2023, Shen *et al.,* 2024, Ye *et al.,* 2024). However, to date, no studies have investigated the role of this gene in the development of the nervous system under normal and pathological conditions using the *Danio rerio* (*D. rerio*) model.

To expand our understanding of the involvement of ANXA2 in the development and functioning of the nervous system, we suppressed the expression of this gene in *D. rerio* at an early stage of ontogenesis. Previously, we demonstrated that suppression of Anxa2a expression in *D. rerio* embryos leads to hydrocephalus at early stages of development (Partevian *et al.,* 2023). To further investigate the role of ANXA2 in nervous system development, we analyzed the effect of Anxa2a suppression on the expression of its key partners (*ahnak*, *egf, egfra, ptena, ptenb, psen1, psen2 and gfap*), which are involved in metabolic processes associated with ANXA2.

[1]National Research Centre “Kurchatov Institute”, 2 Kurchatova Sq., 123182 Moscow, Russia.
[#]These authors contributed equally to this article.

Corresponding Author: Suzanna A. Partevian, National Research Centre “Kurchatov Institute”, 2 Kurchatova Sq., 123182 Moscow, Russia. Email: s.partev@yandex.ru

How to cite this article: Partevian, S.A., Rybolovlev, I.N., Slominsky, P.A., Shadrina, M.I. and Alieva, A.K. (2026). Knockdown of Anxa2a Expression Causes Hydrocephalus in *Danio rerio. Indian Journal of Animal Research*. 1-8. doi: 10.18805/IJAR.BF-2116.

Submitted: 27-02-2026 **Accepted:** 16-04-2026 **Online:** 20-07-2026

MATERIALS AND METHODS

Maintenance of *Danio rerio*

Maintenance of *D. rerio* was performed as described previously (Partevian *et al.,* 2023). The study was conducted in accordance with the ARRIVE 2 guidelines (Percie du Sert

et al., 2020). The whole experiment was carried out in accordance with the European Convention for the Protection of Vertebrate Animals (CETS no. 123) and bioethical norms (https://cioms.ch/images/stories/CIOMS/IGP2012.pdf). Animal experiments were approved by the Ethical Committee of National Research Center "Kurchatov Institute"-IMG (no. 2/19, February 20, 2019).

Design of morpholino oligonucleotides, injection protocol and group formation

The design of the morpholino oligonucleotides (MOs) and the injection protocol were described previously (Partevian *et al.,* 2023). The sequences of MOs are presented in Table 1.

To conduct the study, we formed two groups of fish: a control MO (Co-Mo) group (n = 299) and a group injected with MOs designed to suppress Anxa2a expression (Mo-Anxa2a, n = 290). The Standard Control MOs sequence was selected as the control for MO-related effects on the embryo, in accordance with MO usage recommendations (Eisen and Smith, 2008, Tseng *et al.,* 2016). This sequence does not target any *D. rerio* mRNA sequence and exhibits low biological activity. A total of nine experimental replicates were performed.

Assessment of morphological characteristics in morpholino oligonucleotide injected *D. rerio*

The initial suppression of the *anxa2a* gene expression was evaluated by analyzing phenotypic changes in *D. rerio* organisms. Phenotypic observation was performed using an MC-2-Zoom var. 2 CR microscope (Micromed, Russia). The primary embryotoxic effect was assessed at 2 dpf. The total number of surviving embryos was taken as 100%. In each experiment, the proportions of abnormal fish and fish without phenotypic changes were calculated relative to the number of animals surviving on that day. Mean proportion values were then determined separately for each phenotype. The following types of deformities were identified: anomalies of the head region (enlargement of the HBV, eye and olfactory pit deformities), anomalies of the tail region, notochord development defects and circulatory effects (cardiac and pericardial sac developmental anomalies). Deformities were considered specific if they recurred across all independent experimental replicates and were not observed in the control group. The method for determining the degree of HBV enlargement has been described previously (Partevian *et al.,* 2025).

Total protein extraction

Total protein was extracted from whole fish organisms (including the chorion) in both the Co-Mo and Mo-Anxa2a groups. For this procedure, 20 fish were randomly selected from each group, pooled and resuspended in a solution consisting of 295.5 µl PierceTM RIPA Buffer (Thermo Scientific, USA), 3 µl protease inhibitor (100X Halt™ Protease and Phosphatase Single-Use Inhibitor Cocktail, Thermo Scientific, USA) and 1.5 µl (250 U) DNase (Zymo Research Corp., USA). The samples were homogenized using a Bioprep-6 instrument (Allsheng, China) for 10 cycles of 30 seconds each. Between homogenizations, the samples were cooled on an ice bath for 10 seconds. The homogenate was then centrifuged for 30 minutes at +4°C and 13 200 rpm. Following centrifugation, 20 µl of the supernatant was collected and stored at -20°C for subsequent protein concentration measurement using the Bradford assay. 4x Sample Buffer (1 M Tris-HCl pH 6.5, 1 M DTT, 277 mM SDS, 4.3 M glycerol) was added to the remaining supernatant at a 3:1 ratio and heat denaturation was performed at 95°C (Biosan, Latvia) for 5 minutes. After denaturation, the resulting samples were stored at room temperature for subsequent western blot analysis.

Table 1: Sequences of morpholino oligonucleotides.

Standard control sequence	5′-CCTCTTACCTCAGTTACAATT TATA-3′
anxa2a-start-codon sequence	5′-TCAGAGACCAAAGCCATCC TGGACT-3′

Measurement of protein levels by western blot

In the first stage of the Western blot, 10 µl of isolated protein samples and 2 µl of standard (PageRuler™ Plus Prestained Protein Ladder, Thermo Scientific™, USA) were loaded onto a gradient polyacrylamide gel (Mini-PROTEAN® TGX™ Precast Gels, Any kD, Bio-Rad, USA). The gel was placed in a buffer tank (Mini-PROTEAN® Tetra System, Bio-Rad) containing 1x Running Buffer (25 mM Tris base, 192.4 mM Glycine, 3.47 mM SDS). The stacking phase was carried out at 100 V for 15 minutes and the resolving phase at 200 V for 35 minutes. Upon completion of electrophoresis, the gel was washed three times in distilled water. Following electrophoresis, protein transfer to a polyvinylidene difluoride membrane (Immun-Blot® Low Fluorescence PVDF membrane, Bio-Rad, USA) was performed using Transfer buffer (25 mM Tris base, 190 mM glycine, 20% methanol, pH 8.3) in a Mini Trans-Blot® Electrophoretic Transfer Cell (Bio-Rad, USA) at 90 mA for 16 hours at 4°C. To verify the transfer, the gel was silver stained according to the protocol of Dunigan and Agarkova, (2016). The transfer was considered successful if no protein bands and/or marker bands were visually detectable on the gel. IC Measure software (The Imaging Source, LLC, USA) was used for band visualization. Subsequently, the membrane was incubated with primary antibodies against Anxa2a (Table 2) for 16 hours at 4°C. In the next step, the membrane was incubated with horseradish peroxidase (HRP)-conjugated secondary antibodies (Table 2) for two hours. The chemiluminescent signal was detected using the ChemiDoc MP Imaging System (Bio-Rad, USA) and Image Lab software (Bio-Rad, USA).

To assess the Anxa2a protein expression level, densitometric analysis of the digital images of the PVDF membranes was performed using ImageJ software (Wayne Rasband, USA). Protein levels were normalized to total protein load. The numerical data reflecting the change in protein level are presented in arbitrary densitometric units (ADU).

Total RNA isolation

For total RNA isolation, samples from randomly selected fish at 2 days post-fertilization (dpf) were pooled at a quantity of 10 samples per pool for each group (Co-Mo and Mo-Anxa2a). The RNA isolation procedure was performed using the Direct-Zol MiniPrep kit (Zymo Research Corp, USA) in accordance with the manufacturer's instructions. The concentration of the isolated total RNA was measured using the Quant-iT RNA BR Assay Kit and a Qubit 3.0 fluorometer (Invitrogen, USA). Following isolation, yeast tRNA (at a concentration of 1 mg/ml) was added in a 1:10 ratio (Suslov and Steindler 2005). The samples were subsequently stored at -70°C.

Table 2: Antibodies used for Western blot analysis.

Protein	Molecular weight (kDa)	Manufacturer	Dilution
	Primary antibodies		
Anxa2a	39	Anti-Annexin-2/ANXA2 Rabbit pAb, GB111259-100, Servicebio (China)	1:1000
	Secondary antibodies		
Goat antirabbit IgG H&L (HRP)	-	ab205718, Abcam (USA)	1:10000

Table 3: Oligonucleotide sequences of the primers and TaqMan probes.

Gene	Nucleotide sequence
Nucleotide sequences for housekeeping genes	
aars1	Probe: 5′-VIC-CGCCGCATCCTAGACCGCAAGATCCAG-BHQ2-3′
NM_001044310.2*	Forward primer: 5′-GCACAGTTCCTTAAAACCCTTAGC-3′
	Reverse primer: 5′-AACCGTAGGTGTCATACAGCAG-3′
lsm12b	Probe: 5′-VIC-CGTCGTAATCTCACCACCGTACCAGGT-BHQ2-3′
NM_213148.1	Forward primer: 5′-GGCAGGAGAAGAACATCATTGTGAT-3′
	Reverse primer: 5′-TGTTTGCTGTGCTTGTGAACG-3′
Nucleotide sequences for the target gene *anxa2a*, its main target genes and regulatory genes	
anxa2a	Probe: 5′-VIC-CGCTGGTAATCTCCCTTTGTGTGCTCA-BHQ2-3′
NM_181761.2	Forward primer: 5′-TGGACCTCAAGAAGATCAGACAAG-3′
	Reverse primer: 5′-CAGTTCTCCTCCAATCCTCAGTC-3′
egf	Probe: 5′-VIC-GGCTGCTGGAAACTTCAACTGTGTGG-BHQ2-3′
NM_001365527.1	Forward primer: 5′-CCTGCCGAGGAGGCTTTAT-3′
	Reverse primer: 5′-GAGGTTCATTCTCTGGATGCTATTTC-3′
egfra	Probe: 5′-VIC-GCTTCTTCAGCAGCCCGAGCACG-BHQ2-3′
NM_194424.1	Forward primer: 5′-GTGGACGCAGACGAGTATTTAGT-3′
	Reverse primer: 5′-CACTGGATAACCATTCCCGTTTCTA-3′
ptena	Probe: 5′-VIC-ACAGGAGTGAGGTGAATCCCCAGGG-BHQ2-3′
NM_200708.2	Forward primer: 5′-TCCTCTTCCATAAAATGGTGTTCC-3′
	Reverse primer: 5′-GTGTGGATCTTTACCTTCAACTGAT-3′
ptenb	Probe: 5′-VIC-TCTCTGTGCTCTCCTCTGACCCAGGG-BHQ2-3′
NM_001001822.3	Forward primer: 5′- GACATCAAGGTGGAGTTCTTCCA-3′
	Reverse primer: 5′- CTCTCTGCTGTTTGTATTCCATCCA-3′
gfap	Probe: 5′-VIC-TTGTGCGAACTGTTGAGACCCGTGAC-BHQ2-3′
NM_131373.2	Forward primer: 5′-CCAGCATGGACACTAAACTGAC-3′
	Reverse primer: 5′-GCAGATCCTTCCTCTCCGTAG-3′
ahnak	Probe: 5′-VIC- GTGGAAAACTTCTGGGCTGTGGCAGA-BHQ2-3′
XM_005173182.5	Forward primer: 5′- GAACGAACGAGAGTACACGAATAAG-3′
	Reverse primer: 5′-GCTTCTTCACCTGTCCCCTAG-3′
psen1	Probe: 5′-VIC-GCCACCACCACCAGCAGATGATGAC-BHQ2-3′
NM_131024.1	Forward primer: 5′-GACGACAGATCCAGGAGATGC-3′
	Reverse primer: 5′-CCCACCAGCATACTGTAAAAGATGA-3′
psen2	Probe: 5′-VIC-GTCCGCCTGGGTCATCCTGGG-BHQ2-3′
NM_131514.2	Forward primer: 5′-CGTATCTCATCGTCATCAGTGC-3′
	Reverse primer: 5′-GGAAAATGGGCTCATTTCTTTCTTG-3′

*Accession numbers in the NCBI-GenBank database. VIC – fluorescent dye, BHQ2 – fluorescence quencher.

Selection of primers and TaqMan probes for real-time PCR

The selection of TaqMan primers and probes was performed as described previously (Partevian *et al.,* 2024). The sequences of the selected primers and TaqMan probes are listed in Table 3.

Analysis of changes in the relative expression level of the main Anxa2a partners *s100a10a* and *s100a10b* was not performed. This was due to the inability to select an optimal TaqMan primer and probe system that satisfied the conditions of the approach used in this study. *aars1* and *lsm12b* were used as reference genes (Partevian *et al.,* 2024).

Real-time PCR (qPCR) using TaqMan probes was performed according to the protocol described previously (Partevian *et al.,* 2024). The calculation of relative gene expression levels was carried out using the ΔΔCt threshold cycle comparison method (Rao *et al.,* 2013).

Statistical processing and bioinformatic data analysis

The gene interaction network was constructed using Pathway Studio v. 12.4.0.5 (Elsevier, Netherlands) and STRING (ver. 12.0).

Statistical analysis of the obtained data was performed using the Statistica for Windows 8.0 software package [StatSoft, Inc. (2007), USA] and MS Excel 2019 software (Microsoft, USA). Changes in the relative expression levels of genes at the mRNA and protein level were assessed using the Mann-Whitney U-test.

RESULTS AND DISCUSSION

Based on the results of a previous study (Partevian *et al.,* 2023), the initial phase of the current work involved a detailed phenotypic analysis of *D. rerio* following the suppression of *anxa2a* gene expression by injecting 3 ng of morpholino at 2 days post-fertilization (dpf).

Upon analyzing the phenotype of fish in the Mo-Anxa2a group, the following changes were observed in multiple experimental replicates only in this group: hydrocephalus (enlargement of the hindbrain ventricle (HBV)) and ocular and olfactory pit malformations (Table 4). It should be noted that some fish (30.14%) with specific morphogenesis disruptions in the head region also exhibited developmental abnormalities of the tail and notochord. Furthermore, deformations of the body, tail and notochord (without concomitant specific abnormalities in the head region) were also observed in control and experimental groups, indicating the nonspecificity of the observed phenotype. Therefore, for subsequent expression analysis, we selected individuals with specific head region deformations from the Mo-Anxa2a group and individuals with a normal phenotype from the Co-Mo group.

Next, a detailed analysis of the severity of hydrocephalus was performed in fish with specific deformations using the previously developed approach (Partevian *et al.,* 2025). Two subgroups of fish were identified: those with pronounced (or severely expressed) enlargement of the HBV area (2.49±0.43 fold increase, 42.55% of individuals) and those with mild HBV enlargement area (1.33±0.23 fold increase, 17.73% of individuals) compared to the control group (Fig 1).

Western blot analysis was performed to determine the efficiency of suppressing Anxa2a expression at the translational level using the Morpholino oligonucleotide (MO). The analysis demonstrated that Anxa2a protein expression was reduced twofold in the Mo-Anxa2a group

Table 4: Phenotypic alterations observed in Co-Mo and Mo-Anxa2a groups following Mos injection.

Types of deformations in *D. rerio* (%), 2 dpf, 3 ng			
	Hydrocephalus, ocular and olfactory pit malformations	Nonspecific deformations	Normal phenotype
Co-Mo	0	13.9	86.1
Mo-Anxa2a	52.4	21.9	25.7

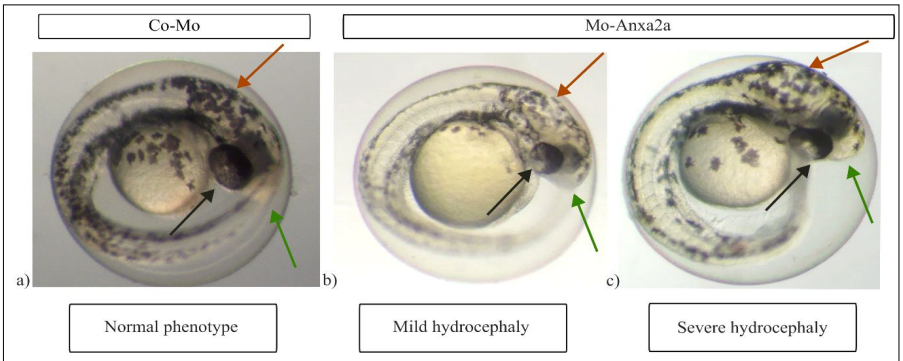

The red arrow indicates the hindbrain ventricle, the green arrow indicates the olfactory pit and the black arrow indicates the eyes. a) Co-Mo - Control morpholino group. b, c) Mo-Anxa2a - group injected with a MO sequence complementary to the start codon region of *anxa2a* mRNA.

Fig 1: Phenotypic changes observed in Co-Mo and Mo-Anxa2a groups following injection of morpholino oligonucleotides.

(Me = 0.17±0.04) compared to the Co-Mo group (Me = 0.36±0.08) at 2 dpf (Fig 2). This reduction confirms the effectiveness of the 3 ng MO injection in suppressing Anxa2a protein expression. Crucially, the expression of this gene did not change statistically at the mRNA level, thereby confirming that the suppression of Anxa2a protein occurs at the translational level.

Then, an analysis of the change in the relative mRNA expression level of the main Anxa2a partner genes (*egf, egfra, ptena, ptenb, gfap, psen1, psen2*) was conducted. The analysis was performed both for the entire Mo-Anxa2a group of fish with specific deformations and separately for fish with pronounced and mild hydrocephalus. The results are presented in Table 5.

As can be seen from Table 5, all groups of fish with suppressed Anxa2a expression exhibited pronounced, statistically significant decrease in the relative expression level of the following genes: *ptena, ptenb, gfap, psen1* and *psen2*. In contrast, no statistically significant changes in the expression of the *ahnak* gene were observed across any of the experimental groups. Furthermore, fish with severe hydrocephalus also showed a decline in the expression of *egf* and *egfra*, suggesting a significant contribution of these genes to the development of severe hydrocephalus.

Currently, there is a growing interest in investigating the role of ANXA2 in nervous system development under both physiological and pathological conditions. However, most studies have been conducted using cell cultures and murine models. In the *D. rerio* model, the roles of the ANXA2 orthologs - Anxa2a and Anxa2b - in nervous system function remain poorly understood (Quoseena *et al.,* 2020). Therefore, the aim of our study was to evaluate the impact of Anxa2a knockdown on nervous system functioning in *D. rerio*.

In the present study, it was demonstrated that suppression of Anxa2a expression at the protein level leads to the development of morphological changes of varying severity in the nervous system of *D. rerio*. Such phenotypic alterations may be associated with the involvement of ANXA2 in a range of biological processes potentially significant for nervous system function. ANXA2 is involved in these processes both independently and through interaction with its primary partners (Partevian *et al.,* 2025).

To gain a more complete understanding of the effect of altered Anxa2a expression on the nervous system of *D.*

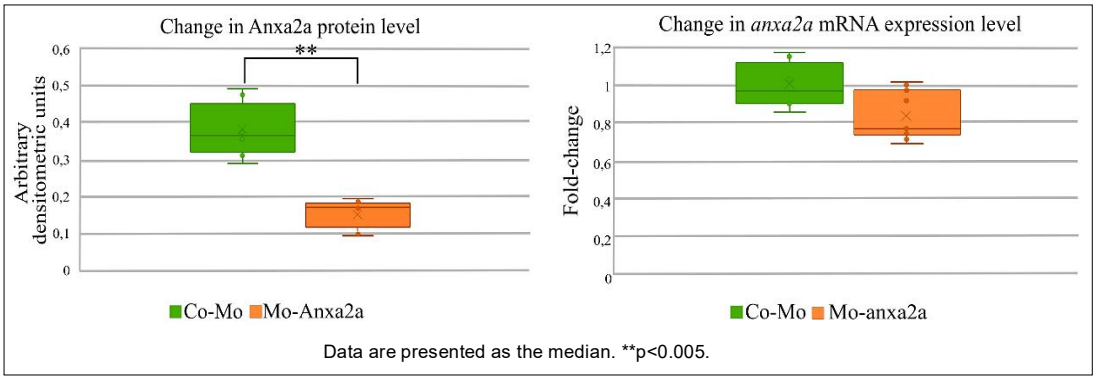

Fig 2: Change in Anxa2a expression at the protein level (a) and mRNA level (b).

Table 5: Results of the analysis of changes in the relative mRNA expression of the main Anxa2a partner gene.

All *D. rerio* exhibiting specific defects							
ahnak	*egf**	*egfra*	*ptena*	*ptenb*	*gfap*	*psen1*	*psen2*
0.90[1]	0.88	0.75	0.50	0.41	0.53	0.46	0.51
0.67-1.11[2]	0.81-0.97	0.53-0.85	0.43-0.55	0.39-0.45	0.45-0.63	0.36-0.52	0.48-0.54
***D. rerio* with pronounced hydrocephalus**							
ahnak	*egf*	*egfra*	*ptena*	*ptenb*	*gfap*	*psen1*	*psen2*
0.94	0.80	0.54	0.42	0.40	0.44	0.43	0.48
0.80-1.16	0.78-0.86	0.48-0.77	0.40-0.48	0.37-0.44	0.43-0.46	0.34-0.51	0.47-0.49
***D. rerio* with mild hydrocephalus**							
ahnak	*egf*	*egfra*	*ptena*	*ptenb*	*gfap*	*psen1*	*psen2*
0.79	0.95	0.85	0.57	0.49	0.66	0.46	0.54
0.56-1.01	0.89-1.03	0.77-0.99	0.51-0.68	0.46-0.54	0.56-0.73	0.43-0.54	0.53-0.61

[1]Fold-change of median. [2]25th–75th percentiles. *Statistically significant results ($p<0.05$) are highlighted in color. The expression level in the Co-Mo group was set to 1.

rerio, we carried out a selection of the main partners (proteins and their encoding genes) of Anxa2a using the Pathway Studio v.12.4.0.3 program. This analysis enabled the identification of 31 ANXA2 partners. These partners were analyzed for compliance with the following criteria: interaction with ANXA2 shown in at least two separate publications, association with neurological diseases and/or expression in the nervous system and presence of orthologs in *D. rerio*. Ultimately, we identified six partners that satisfied all three conditions, namely, GFAP (Gfap), EGFR (Egfra), PTEN (Ptena and Ptenb), EGF (Egf) and S100A10 (S100a10a and S100a10b) and AHNAK (Ahnak). PSEN1 (Psen1) and PSEN2 (Psen2) satisfy two of the three criteria: they are associated with Alzheimer's disease and have orthologs in fish. Furthermore, it has been previously shown that suppression of *psen1* and *psen2* gene expression by MO in *D. rerio* results in the development of hydrocephalus (Nornes *et al.,* 2009). In addition, an interaction between PSEN1 and ANXA2 was demonstrated in the study by Bustos *et al.* (2017). Consequently, these genes were also included in our subsequent expression analysis.

Further analysis of the Anxa2a partners using the STRING resource (v. 12.0) indicates close regulatory interactions among the selected partners.

As shown in Fig 3, Egf and Egfra are targets regulated by Anxa2a. Based on the data presented in Table 5, a statistically significant decrease in *egf* and *egfra* expression was observed in the overall Mo-Anxa2a group, as well as in *D. rerio* with severe hydrocephalus. The most pronounced drop in expression was observed for the *egfra* gene. Based on this finding, it can be hypothesized that *egfra* makes a direct contribution to the development of the morphological changes we observed, which are associated with nervous system development. These changes may be linked to the fact that ANXA2 is involved in the clathrin-dependent internalization of EGFR at the cell membrane and promotes the activation of its downstream signaling pathways (Grewal and Enrich, 2009; Chaudhary *et al.,* 2014).

It has also been shown in *D. rerio* that the activation of the MAPK/ERK signaling pathway *via* HB-EGF/EGFR is essential for the proliferation of basal cells and the restoration of olfactory epithelium neurogenesis after injury (Sireci *et al.,* 2024). These data indirectly support our findings. It can be hypothesized that the olfactory pit deformations we observed may be linked to the disruption of the PI3K/Akt and MAPK/ERK signaling pathways, where EGFR is an important participant. We hypothesize that the decrease in Anxa2a expression might impair EGFR internalization and its subsequent intracellular vesicular transport within the cell. The accumulation of EGFR on the cell surface then leads to a reduction in its mRNA level.

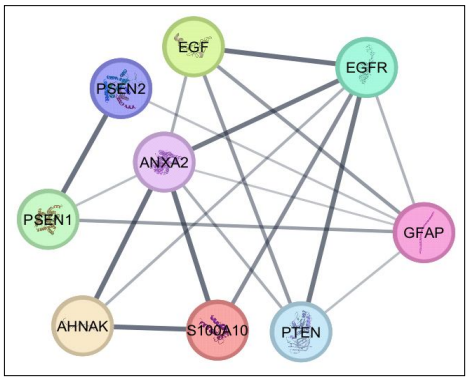

Fig 3: Interaction network between ANXA2 and its main partners (STRING v. 12.0).

Furthermore, a slight but significant decrease in the expression of the main ligand of *egfra* - *egf* was also observed in the group with severe hydrocephalus. It is possible that such a decrease in expression may lead to the disruption of metabolic processes associated with cell division, thereby contributing to the formation of severe hydrocephalus.

In *D. rerio* developing hydrocephalus, a decrease in the expression of the *ptena* and *ptenb* genes was observed. The PTEN protein (orthologs in *D. rerio:* Ptena and Ptenb) is part of the same signaling pathway as the EGF, EGFR and ANXA2 proteins (Castaldo *et al.,* 2019). Previously, Croushore *et al.,* (2005) investigated the expression patterns of *ptena* and *ptenb* in *D. rerio* under normal and pathological conditions. It was demonstrated that *ptena* and *ptenb* expression in *D. rerio* is most pronounced in the central nervous system, eyes, pharyngeal arches and pectoral fins by 48 hours post fertilization (Croushore *et al.,* 2005). Despite similar distribution patterns within the organism, distinct phenotypes were observed upon the suppression of these proteins. Specifically, Ptena knockdown led to deformations in the head and notochord regions, as well as impaired vasculogenesis and otolith development. Conversely, Ptenb knockdown was associated with brain ventricle enlargement (domed head, hydrocephalus), as well as tail and yolk deformations (Croushore *et al.,* 2005). It is possible that the suppression of *anxa2a* gene expression leads to the formation of a specific phenotype via the downregulation of *ptena* and *ptenb* and the activation of the PI3K/Akt pathway, followed by the development of oxidative stress. For instance, reduced *ptena* expression may result in otolith and tail deformations, while reduced *ptenb* expression may lead to ventricular enlargement, a finding confirmed by previous independent studies. However, this hypothesis requires further experimental validation.

A decrease in the expression of *psen1* and *psen2* genes was also observed in both groups. It is noteworthy that PSEN1, in conjunction with ANXA2, participates in autophagosome formation and the subsequent cleavage of amyloid-beta (Bustos *et al.,* 2017). Furthermore, PSEN1, as a component of the γ-secretase complex, is involved in the processing of the Notch protein (Hurley *et al.,* 2023). A previously published independent study demonstrated that the suppression of Psen1 and Psen2 expression using MOs in *D. rerio* resulted in the development of hydrocephalus and a reduction in melanocyte number (Nornes *et al.,* 2009). Based on these findings, it can be hypothesized that the downregulation of Anxa2a may indirectly lead to the development of

hydrocephalus *via* the reduction of *psen1* and *psen2* expression. Such changes in expression may lead to further disruption of autophagy, the Notch signaling pathway and the formation of a specific phenotype.

A statistically significant decrease in the relative mRNA levels of the *gfap* gene, which encodes the glial fibrillary acidic protein (Gfap), was identified in all groups. This protein is a constituent of intermediate filaments in astrocytes. It is known that ANXA2 is also expressed in astrocytes and can regulate their proliferation (Chen *et al.,* 2017). Previous studies have shown that ANXA2 can interact with GFAP and promote its assembly into glial filaments in a Ca^{2+}-dependent manner (Garbuglia *et al.,* 1995). We hypothesize that the reduction in *gfap* expression, coupled with the inhibition of Anxa2a translation, impairs the assembly of glial filaments. This disruption of astrocyte function may serve as a primary mechanism underlying the development of inflammatory hydrocephalus.

Also, no statistically significant decrease in the expression of the *ahnak* gene, whose protein product forms a complex with Anxa2a, was observed in either group (Jin *et al.,* 2020). Possibly, this is due to the fact that the metabolic pathways jointly involving Anxa2a and Ahnak are not implicated in the development of hydrocephalus.

Thus, the data obtained suggest that an altered Anxa2a level may lead to pathological processes in the nervous system and the development of hydrocephalus through the modification of metabolic pathways associated with its main partners: *egf* and *egfra* (cell division), *ptena* and *ptenb* (reactive oxygen species formation), *psen1* and *psen2* (autophagy) and *gfap* (regulation of inflammation in astrocytes). However, this remains a hypothesis and requires further research to be fully validated.

CONCLUSION

Despite the extensive research on the role of ANXA2 in the pathogenesis of neurodegenerative diseases, no studies have yet been published investigating this protein's role in nervous system development using the *D. rerio* model. In the present study, we demonstrate for the first time that altering Anxa2a expression levels leads to pathological processes in the nervous system, specifically the development of hydrocephalus. This was accompanied by a statistically significant change in the mRNA expression levels of key Anxa2a interactors: e*gf, egfra, ptena, ptenb, gfap, psen1* and *psen2*. Thus, it can be hypothesized that the observed effects are mediated through the disruption of key biological processes: cell division (via *egf* and *egfra*), reactive oxygen species production (via *ptena* and *ptenb*), autophagy (*via psen1* and *psen2*) and the regulation of inflammation (*via gfap*).

However, the involvement of these signaling pathways needs to be confirmed in larger sample sizes using a comprehensive approach that incorporates both transcriptomic and proteomic profiling.

ACKNOWLEDGEMENT

Funding

The work was performed within the framework of the state assignment of the National Research Center Kurchatov Institute (1F.6.1).

Institutional review board statement

Animal experiments were approved by the Ethical Committee of National Research Center "Kurchatov Institute"-IMG (no. 2/19, February 20, 2019).

Conflict of interest

The authors declare no conflicts of interest.

REFERENCES

Bharadwaj, A., Bydoun, M., Holloway, R. and Waisman, D. (2013). Annexin A2 heterotetramer: Structure and function. *Int. J. Mol. Sci.* **14(3):** 6259-6305.

Bustos, V., Pulina, M.V., Bispo, A., Lam, A., Flajolet, M., Gorelick, F.S. and Greengard, P. (2017). Phosphorylated Presenilin 1 decreases beta-amyloid by facilitating autophagosome-lysosome fusion. *Proc. Natl. Acad. Sci. U S A.* **114(27):** 7148-7153.

Castaldo, S.A., Ajime, T., Serrao, G., Anastacio, F., Rosa, J.T., Giacomantonio, C.A., Howarth, A., Hill, R. and Madureira, P.A. (2019). Annexin A2 regulates AKT Upon H_2O_2-Dependent signaling activation in cancer cells. *Cancers (Basel).* **11(4):** 492.

Chaudhary, P., Thamake, S.I., Shetty, P. and Vishwanatha, J.K. (2014). Inhibition of triple-negative and Herceptin-resistant breast cancer cell proliferation and migration by Annexin A2 antibodies. *Br J. Cancer.* **111(12):** 2328-2341.

Chen, J., Cui, Z., Yang, S., Wu, C., Li, W., Bao, G., Xu, G., Sun, Y., Wang, L. and Zhang, J. (2017). The upregulation of annexin A2 after spinal cord injury in rats may have implication for astrocyte proliferation. *Neuropeptides.* **61:** 67-76.

Croushore, J.A., Blasiole, B., Riddle, R.C., Thisse, C., Thisse, B., Canfield, V.A., Robertson, G.P., Cheng, K.C. and Levenson, R. (2005). Ptena and ptenb genes play distinct roles in zebrafish embryogenesis. *Dev Dyn.* **234(4):** 911-921.

Dunigan, D. and Agarkova, I. (2016). Silver Development protocol (silver stain) for 0.75 mm polyacrylamide gels. *protocols.io.* https://dx.doi.org/10.17504/protocols.io.ermbd46.

Eisen, J.S. and Smith, J.C. (2008). Controlling morpholino experiments: Don't stop making antisense. *Development.* **135(10):** 1735-1743.

Garbuglia, M., Bianchi, R., Verzini, M., Giambanco, I. and Donato, R. (1995). Annexin II2-p11(2) (calpactin I) stimulates the assembly of GFAP in a calcium- and pH-dependent manner. *Biochem. Biophys. Res. Commun.* **208(3):** 901-909.

Grewal, T. and Enrich, C. (2009). Annexins-modulators of EGF receptor signalling and trafficking. *Cell Signal.* **21(6):** 847- 858.

Grindheim, A.K., Saraste, J. and Vedeler, A. (2017). Protein phosphorylation and its role in the regulation of Annexin A2 function. *Biochim Biophys Acta Gen Subj.* **1861(11 Pt A):** 2515-2529.

Hurley, E.M., Mozolewski, P., Dobrowolski, R. and Hsieh, J. (2023). Familial Alzheimer's disease-associated PSEN1 mutations affect neurodevelopment through increased Notch signaling. *Stem Cell Reports*. **18(7):** 1516-1533.

Jin, J., Bhatti, D.L., Lee, K.W., Medrihan, L., Cheng, J., Wei, J., Zhong, P., Yan, Z., Kooiker, C., Song, C., Ahn, J.H., Obermair, G.J., Lee, A., Gresack, J., Greengard, P. and Kim, Y. (2020). Ahnak scaffolds p11/Anxa2 complex and L-type voltage-gated calcium channel and modulates depressive behavior. *Mol. Psychiatry.* **25(5):** 1035-1049.

Mawolo, J.B. and Akiti, C.J.A.R. (2021). Comparative study of the distribution and localization of neuroglobin expression in the mammalian brain: A literature review. *Agricultural Reviews*. **42(4):** 359-370. doi: 10.18805/ag.R-153.

Nornes, S., Newman, M., Wells, S., Verdile, G., Martins, R.N. and Lardelli, M. (2009). Independent and cooperative action of Psen2 with Psen1 in zebrafish embryos. *Exp. Cell Res.* **315(16):** 2791-2801.

Partevian, S.A., Rybolovlev, I.N., Slominsky, P.A., Shadrina, M.I. and Alieva, A.K. (2025). Assessment of hydrocephalus severity in *Danio rerio* at an early developmental stage. *Vestnik Voennogo innovacionnogo tekhnopolisa «ERA»* **6:** 263-265.

Partevian, S.A., Safina, D.R., Rudenok, M.M., Rybolovlev, I.N., Semenova, E.I., Shadrina, M.I., Slominsky, P.A., Kostrov, S.V. and Alieva, A.K. (2023). The effect of morpholino oligonucleotides to gene ANXA2a on the embryonic development of *Danio rerio*. *Molecular Genetics, Microbiology and Virology.* **38(3):** 143-149.

Partevian, S.A., Safina, D.R., Rybolovlev, I.N., Rudenok, M.M., Kostrov, S.V., Shadrina, M.I., Slominsky, P.A. and Alieva, A.K. (2024). Screening and stability analysis of housekeeping genes for transcriptomic studies in *Danio rerio* (Zebrafish) at early developmental stages. *Molecular Genetics, Microbiology and Virology*. **39(2):** 131-136.

Partevian, S.A., Slominsky, P.A., Shadrina, M.I. and Alieva, A.K. (2025). ANXA2 protein and its role in neurodegeneration processes. *Life (Basel)*. **15(3):** 402.

Percie du Sert, N., Hurst, V., Ahluwalia, A., Alam, S., Avey, M.T., Baker, M., Browne, W.J., Clark, A. *et al.* (2020). The ARRIVE guidelines 2.0: Updated guidelines for reporting animal research. *PLoS Biol.* **18(7):** e3000410.

Quoseena, M., Vuppaladadium, S., Hussain, S., Banu, S., Bharathi, S. and Idris, M.M. (2020). Functional role of annexins in zebrafish caudal fin regeneration - A gene knockdown approach in regenerating tissue. *Biochimie.* **175:** 125-131.

Rao, X., Huang, X., Zhou, Z. and Lin, X. (2013). An improvement of the 2^(-delta delta CT) method for quantitative real-time polymerase chain reaction data analysis. *Biostat. Bioinforma Biomath.* **3(3):** 71-85.

Rudenok, M.M., Shadrina, M.I., Filatova, E.V., Rybolovlev, I.N., Nesterov, M.S., Abaimov, D.A., Ageldinov, R.A., Kolacheva, A.A., Ugrumov, M.V., Slominsky, P.A. and Alieva, A.K. (2022). Expression analysis of genes involved in transport processes in mice with MPTP-induced model of Parkinson's disease. *Life (Basel).* **12(5):** 751.

Shen, Y., Ma, C., Li, X., Li, X., Wu, Y., Yang, T., Hu, Y., Liu, C., Shen, H., Guo, P. and Shen, Y. (2024). Generation of B7-H3 isoform regulated by ANXA2/NSUN2/YBX1 axis in human glioma. *J Cell Mol. Med.* **28(14):** e18575.

Sireci, S., Kocagoz, Y., Alkiraz, A.S., Guler, K., Dokuzluoglu, Z., Balcioglu, E., Meydanli, S., Demirler, M.C., Erdogan, N.S. and Fuss, S.H. (2024). HB-EGF promotes progenitor cell proliferation and sensory neuron regeneration in the zebrafish olfactory epithelium. *FEBS J.* **291(10):** 2098-2133.

Suslov, O. and Steindler, D.A. (2005). PCR inhibition by reverse transcriptase leads to an overestimation of amplification efficiency. *Nucleic Acids Res.* **33(20):** e181.

Tseng, L.C., Tang, C.H. and Jiang Y.J. (2016). Morphology and gene expression screening with morpholinos in zebrafish embryos. *Methods Mol. Biol.* **1470:** 213-224.

Ye, L., Zhao, J., Xiao, Z., Gu, W., Liu, X., Ajuyo, N.M.C., Min, Y., Pei, Y. and Wang, D. (2024). Integrative human genetic and cellular analysis of the pathophysiological roles of anxa2 in alzheimer's disease. *Antioxidants (Basel)*. **13(10):** 1274.

Zhang, S., Jiang, C., Su, Y., Gui, J., Yue, Z., Jian, B., He, S. and Ma, X. (2023). Nectin2 influences cell apoptosis by regulating ANXA2 expression in neuroblastoma. *Acta Biochim. Biophys Sin (Shanghai)*. **55(3):** 356-366.